A novel NLR immune receptor from Aegilops tauschii confers resistance to wheat eyespot disease

Sanu Arora

Sanu.Arora@jic.ac.uk

John Innes Centre https://orcid.org/0000-0002-6632-2171

David Gilbert

King Abdullah University of Science and Technology

Kumar Gaurav

John Innes Centre

Nicolas Trenk

John Innes Centre https://orcid.org/0000-0003-3328-6888

Alberto Prieto

RAGT Seeds Ltd.

Clare Moscrop

RAGT Seeds Ltd.

Andrew Steed

John Innes Centre

Tom O'Hara

John Innes Centre

Alba Pacheco-Moreno

John Innes Centre

Mishi Vachev

John Innes Centre

Samuel Bruty

John Innes Centre https://orcid.org/0009-0009-5395-4573

Sadiye Hayta

JIC https://orcid.org/0000-0003-2920-4720

Mark Smedley

John Innes Centre https://orcid.org/0000-0002-6162-4795

Rose McNelly

John Innes Centre

Paul Nicholson

John Innes Centre https://orcid.org/0000-0002-6458-8697

Ruth Bryant

RAGT Seeds Ltd.

Article

Keywords:

Posted Date: January 2nd, 2026

DOI: https://doi.org/10.21203/rs.3.rs-8021535/v1

Additional Declarations: There is **NO** Competing Interest.

Abstract

Eyespot, a stem-base soil-borne fungal disease, is an important constraint on wheat production in temperate regions. Resistance in wheat remains limited, with *Pch1* and *Pch2* being currently deployed in breeding but no underlying or associated gene identified to date. Here, we phenotyped a sequence-configured diversity panel of *Aegilops tauschii*, the D subgenome progenitor of bread wheat, with one of the two causative agents of eyespot, *Oculimacula yallundae*. A *k*-mer-based genome-wide association mapping approach identified *Pch4*, a nucleotide-binding leucine-rich repeat (NLR) gene on chromosome 1DS. Transgenic wheat and synthetic hexaploids carrying *Pch4* showed strong resistance to the pathogen. Phylogenetic and synteny analyses revealed that *Pch4* belongs to the same NLR lineage as the cereal powdery mildew resistance gene *Pm3*, indicating a shared evolutionary origin. The discovery of *Pch4* expands the repertoire of available eyespot resistances and provides new opportunities for strategic stacking of resistance genes to enhance disease resilience in wheat.

Introduction

Two soil-borne pathogens of wheat, *Oculimacula yallundae* and *Oculimacula acuformis*, cause cereal eyespot, a stem-base disease prevalent in temperate regions[1]. When infected, susceptible wheat varieties can develop moderate to severe stem lesions that disrupt water and nutrient transport, leading to symptoms such as lodging and premature grain ripening, which can cause yield losses of up to 40%[2,3,4]. The two pathogens differ in fungicide response[5] and host preference, with *O. yallundae* being more aggressive on wheat than rye while *O. acuformis* exhibits similar aggressiveness on both hosts[6]. Furthermore, wheat landraces and wild relatives are reported to have differential resistance to the two pathogens, suggesting that resistance to *O. yallundae* and *O. acuformis* may have partially independent genetic mechanisms[7,8].

To date, only a few resistance loci - *Pch1*, *Pch2*, *Pch3* and *QPch.jic-5A* - effective against eyespot have been identified[9,10,11,12,13]. *Pch1*, introgressed onto chromosome 7D from the wheat wild relative *Aegilops ventricosa*, is effective against both *Oculimacula* species and is widely deployed. However, its application has been hindered by linkage drag due to limited recombination within the translocated *Ae. ventricosa* segment[14]. *Pch2* and *QPch.jic-5A* were both identified in the wheat variety Cappelle Desprez. *Pch2* was found to provide effective resistance to *O. acuformis* at the seedling stage but a significantly lower resistance to *O. yallundae*, while *QPch.jic-5A* conferred resistance to both species at both seedling and adult stages[2,13]. *Pch3*, identified on chromosome 4V in *Dasypyrum villosum*, is yet to be widely deployed, likely due to the undesirable linkage drag[11]. Although the screening of multiple wheat and wild wheat diversity panels has revealed promising variation for eyespot resistance, it has not led to identification and deployment of any additional resistance loci[2,15,16,17,18,19].

Wheat wild relatives are a rich, largely untapped, source of disease resistance (*R*) genes for improving the resilience of bread wheat against biotic threats. Analysis of the reported *R* genes for wheat diseases

reveal that over 40% of them have originated from wild species[20]. Among these, *Aegilops tauschii*, the progenitor of wheat D subgenome, stands out as a major contributor. Harnessing its genetic diversity has therefore become a key focus in wheat breeding programs. This wild species comprises three distinct genetic lineages - L1, L2 and L3 - with L2 being the primary donor to the wheat D subgenome[21]. Of the 24 *Ae. tauschii R* genes identified to date that confer resistance to pathogens, 15 have been cloned, all of which confer resistance to foliar diseases (Supplementary Table 1). Although *Ae. tauschii* is also reported to harbour resistance against soil-borne pathogens infecting wheat, no *R* genes underlying such resistance have yet been identified[19].

In this study, we investigate the *Ae. tauschii* genetics underlying resistance to *O. yallundae*. We report the cloning of the first *R* gene conferring resistance to wheat eyespot, a nucleotide-binding domain and leucine-rich repeat (NLR) gene, designated *Pch4*. We discovered this *R* gene by screening a sequence-configured *Ae. tauschii* diversity panel with the pathogen, followed by *k*-mer based genome-wide association study (GWAS). We further demonstrate through synthetic hexaploid phenotyping and transgenic overexpression in a susceptible wheat cultivar that this wild wheat *R* gene provides effective resistance to *O. yallundae* in a hexaploid wheat background. With the cloning of the first *R* gene against a soil-borne disease in *Ae. tauschii*, this work provides a roadmap for further exploration of resistance to soil-borne pathogens of wheat from the D subgenome progenitor.

Results

Association mapping identified eyespot resistance locus on chromosome 1DS

We undertook glasshouse-based phenotyping of a diversity panel consisting of 151 *Ae. tauschii* L2 lines, using a single isolate of *O. yallundae*, 20/848, which was isolated by RAGT Seeds from soil near Cambridge, UK. We adapted an existing phenotyping protocol to screen the *Ae. tauschii* diversity panel along with wheat control lines across three experimental repeats and developed an *Ae. tauschii* specific disease severity scale (Fig. 1a)[22].

Phenotypic analysis revealed that 32 *Ae. tauschii* lines, 21.3% of the diversity panel, exhibited a strong resistance response, out of which 23 lines exhibited greater resistance than the most resistant hexaploid wheat control, *Skyfall*, which carries *Pch1* (Fig. 1b). An additional 14 lines were categorized as having an intermediate response. Notably, several wheat control varieties carrying either *Pch1* or *Pch2* were classified as intermediate or susceptible in this assay indicating that these resistances are not equally effective in all backgrounds (Supplementary Table 2).

We conducted *k*-mer based GWAS using the average phenotype scores of the L2 lines which were sequenced in a previous study[21], except those with intermediate phenotype, and mapped the significantly associated *k*-mers to the reference assembly of TA1675[23]. This mapping revealed a significantly associated peak of 0.7 Mb on chromosome 1DS spanning a region of 6.23 Mb to 6.93 Mb within which there were 12 annotated genes (Fig. 1c-d, Supplementary Table 3). Out of these genes, the

most significantly associated *k*-mers mapped to **Aet.TA1675.r1.1D001090** (Fig. 1d), which belongs to the NLR gene family typically associated with disease resistance in plants. There was only one other NLR gene in the associated interval, **Aet.TA1675.r1.1D001100**, which is located next to **Aet.TA1675.r1.1D001090** at a genomic distance of around 68 kb. We considered both these NLRs as potential candidates underlying the identified eyespot resistance.

Comparison of the two NLR genes showed they shared 82.9% nucleotide identity (Fig. 2a) and 77.7% pairwise amino acid identity (Supplementary Fig. 1). We checked for the presence of both the NLRs across the L2 diversity panel using BLASTn[24]. Despite their physical proximity, the two genes are not perfectly linked and show differential correlation with the phenotype (Fig. 2b-d). **Aet.TA1675.r1.1D001090** was present in 29 of 32 lines scored as resistant along with six intermediate lines and three susceptible lines, while **Aet.TA1675.r1.1D001100** was present in only 16 resistant, seven intermediate and nine susceptible lines, therefore, exhibiting a significantly weaker association with resistance (Supplementary Table 4). Therefore, we focused on **Aet.TA1675.r1.1D001090** as the primary candidate gene for the identified eyespot resistance, hereby designated as *Pch4*.

Based on the RNA-seq mapping to the annotated reference assembly of TA1675 and using InterPro[25], the *Pch4* candidate was ascertained to encode a 1447 amino acid sequence across two exons, with defined coiled-coil (CC), nucleotide-binding (NB), and leucine-rich repeat (LRR) domains (Fig. 2e). The alternate allele in the susceptible line AL8/78, annotated as **AET1Gv20020600**, was found to differ significantly from the *Pch4* candidate, with the two alleles sharing only 85% amino acid identity (Supplementary Fig. 2).

We assessed the broader effectiveness of *Pch4* resistance using historical data, where a single isolate of *O. yallundae*, P84-8, was used to phenotype a diversity collection of *Ae. tauschii* lines[19]. Out of 78 *Ae. tauschii* L2 lines shared with our diversity panel, 18 were ascertained to carry *Pch4* based on the sequencing data, and all of them but one were reported to be resistant, indicating the potential effectiveness of *Pch4* against P84-8 (Supplementary Fig. 3, Supplementary Table 5). We also checked the presence of the *Pch4* candidate in 117 diverse *Ae. tauschii* L1 lines using BLASTn[24] and found four that carry the allele (Supplementary Fig. 4a). L1 lines were screened with a single isolate of *O. yallundae*, 16/847, and all four L1 lines ascertained to carry *Pch4* exhibited a strong resistance response (Supplementary Fig. 4b, Supplementary Table 6).

Validation and characterisation of *Pch4* in hexaploid wheat and *Ae. tauschii*

To assess the potential relevance of *Pch4* for wheat breeding programs, we first examined its allelic variation within the Watkins collection, a recently published diversity panel of wheat landraces sequenced using resistance gene enrichment sequencing[26]. A BLASTn[24] search across 300 lines of this collection failed to identify any wheat lines carrying the *Pch4* candidate allele, suggesting that this allele was likely not introduced into hexaploid wheat during the hybridisation of *Ae. tauschii* with tetraploid wheat.

Next, we ascertained the presence of *Pch4* in synthetic hexaploid wheat (SHW) lines previously generated through direct hybridisation of *Ae. tauschii* D subgenome donors with tetraploid wheat[21] (Supplementary Table 7). We selected two contrasting lines for evaluation, both sharing a highly susceptible tetraploid donor, Hoh-506. The D subgenome donor of SHW-070 was a resistant *Ae. tauschii* accession carrying the *Pch4* candidate allele, while that of SHW-042 was a susceptible *Ae. tauschii* accession carrying an alternate allele. To compare the effectiveness of *Pch4* relative to other known eyespot resistances, we phenotyped the SHWs alongside wheat varieties carrying either *Pch1* (VPM1) or a combination of *Pch2* and *QPch.jic-5A* (Cappelle Desprez) (Fig. 3a, Supplementary Table 8). Phenotyping using a mixed inoculum of *O. yallundae* demonstrated that *Pch4* conferred equally effective resistance in hexaploid wheat as in diploid *Ae. tauschii*. The degree of resistance provided by *Pch4* was comparable to that of *Pch1* and significantly greater than the resistance conferred by the combined *Pch2* and *QPch.jic-5A* (Fig. 3b, Supplementary Table 9).

To determine the inheritance pattern of *Pch4*, a biparental *Ae. tauschii* F_2 population was generated by crossing the resistant line BW_01185, carrying *Pch4*, with the susceptible line BW_01086 that contains an alternate allele. Four F_1 plants were advanced to F_2, generating a total of 164 F_2 seedlings, which were phenotyped in a growth cabinet bioassay using a mixed isolate inoculum of *O. yallundae*. Phenotypic data, and genotypic screening of recombinants using KASP markers designed to distinguish between parental alleles (Supplementary Tables 10 and 11), suggested that resistance is inherited in a dominant manner. Heterozygotes exhibited significantly reduced disease severity compared to the susceptible parent, however, the homozygotes displayed a significantly higher degree of resistance compared to both heterozygotes and homozygotes with the BW_01086 *Pch4* allele, indicating a dosage dependent or incomplete dominance effect (Fig. 3c). To further validate the dosage dependent effect, we tested our homoeolog-specific KASP marker in a SHW backcross (SHWBC) population, NIAB-SHW-BC-219, which was generated by crossing the *Pch4* carrying SHW-069 with the susceptible wheat variety Robigus[27]. The response of the SHWBC population to pathogen infection confirmed a dosage effect for *Pch4*, with homozygotes exhibiting significantly greater resistance than heterozygotes (Supplementary Fig. 5, Supplementary Table 12).

To validate the function of the *Pch4* candidate, we cloned its genomic sequence for stable transgenic expression in the susceptible wheat line Chinese Spring (CS) and placed it in a construct under the control of a rice actin promoter (*OsActin1*) and a 35S terminator (Fig. 3d). We obtained two positive independent T_0 lines carrying *Pch4*, which were advanced to T_2 for phenotyping. We designed a homoeologue specific KASP marker (Supplementary Table 10) to develop sister lines from the same T_0 transgenic that were positive or negative for the presence of *Pch4*. Chinese Spring is highly susceptible to eyespot and therefore any reduction in phenotype score could be attributed to the presence of the transgene. Infection of T_2 plants using a mixed inoculum of *O. yallundae* revealed that the lines containing the transgene were significantly more resistant to eyespot compared to zero copy plants (Fig. 3e-f). To test whether *Pch4* confers species-specific resistance, we infected plants from the T_2 sister lines with a mixed inoculum of *O. acuformis*. Both control and *Pch4* positive lines exhibited a

highly susceptible response, showing that *Pch4* confers species-specific resistance to *O. yallundae* (Supplementary Table 13).

A browning of the coleoptile was frequently observed in the resistant *Ae. tauschii*, SHW and transgenic plants, likely reflecting a phenolic response to pathogen infection. To further validate that our visual phenotyping, based on pathogen penetration and stem lesion development through the successive plant tissue layers, accurately reflected pathogen infection, we employed fluorescence microscopy. Wheat Germ Agglutinin Alexa Fluor® 488 conjugate (WGA-AF-488) was used to visualize the fungal chitin upon excitation, enabling the detection of the pathogen within infected stem tissue. This analysis confirmed clear fungal presence in susceptible *Ae. tauschii* and wheat genotypes, while resistant genotypes had little to no detectable pathogen presence (Supplementary Fig. 6).

Phylogenetic and syntenic analysis suggests an evolutionary link between *Pch4* and *Pm3*, a powdery mildew resistance gene

To explore the evolutionary relationship between *Pch4* and other known NLR genes, we used RefPlantNLR and the NLRtracker pipeline to compare *Pch4* and all NLRs within the reference genome assembly TA1675 with an experimentally validated NLR dataset[28]. *Pch4* and several closely linked genes were observed to cluster with the *Pm3* allelic series and its orthologs *Pm8* and *TmPm3* from rye (*Secale cereale*) and *Triticum monoccocum*, respectively (Fig. 4a-b). These genes convey resistance to the foliar disease powdery mildew (*Blumeria graminis f. sp. Tritici*) and notably, are all located on the short arm of chromosome 1 in their respective species[29,30]. We therefore investigated the synteny of this locus across multiple grass species. We extracted a 4.64 Mb region surrounding *Pch4* from *Ae. tauschii* accession TA1675 and aligned it to the reference genomes of wheat (*Triticum aestivum*), rye (*S. cereale*), *T. monococcum* and barley (*Hordeum vulgare*), which indicated broad conservation of the locus across species (Fig. 4c). *Pch4* shares homology with several *Pm3* orthologs, with pairwise amino acid identities of 73.6%, 77.5% and 78% with *TmPm3*, *Pm8* and *Pm3b* respectively suggesting a shared ancestral origin (Fig. 4d). The expansion and diversification of *Pm3* orthologs across these genomes may have contributed to neofunctionalization as indicated by the distinct disease resistance functions of *Pm3* and *Pch4*.

Genomics-assisted selection of pre-breeding germplasm for *R* gene pyramiding

We compiled a list of all currently cloned *R* genes derived from *Ae. tauschii* L2, encompassing 14 resistance genes against foliar pathogens and one (*Cmc4*) conferring pest resistance. Using sequencing data for the L2 diversity panel, we predicted the presence of these *R* genes, alongside *Pch4*, across accessions (Fig. 5). Notably, *Pch4* was predicted in 48 *Ae. tauschii* accessions, including four previously utilized as D subgenome donors in SHW lines.

This resource will enable an informed selection of germplasm for the development of pre-breeding material enriched with resistance to multiple diseases, facilitating efficient introgression into elite wheat cultivars. For instance, SHW-143, derived from *Ae. tauschii* accession BW_01140, harbours seven cloned

R genes conferring resistance to six diseases: *Pch4, Stb16q, Rwt4, WTK4, Sr46, Sr66* and *Yr28.* The deployment of this SHW in breeding pipelines presents a valuable opportunity to introduce a suite of agronomically important *R* genes in a single breeding cycle.

Discussion

Eyespot is an economically important stem-base disease of wheat caused by two closely related soil-borne fungal pathogens, *O. yallundae* and *O. acuformis*[1,31]. Most commercial wheat cultivars exhibit only partial resistance, typically attributed to the *Pch2* locus, which provides moderate resistance against both species but is more effective against *O. acuformis*[31]. Other known resistance sources include *Pch1*, introgressed from *Ae. ventricosa*, and a QTL on chromosome 5A; however, both suffer from undesirable linkage drag that complicates their use in breeding[9,11]. The lack of cloned eyespot resistance genes has limited precision breeding efforts, leaving elite germplasm particularly vulnerable to *O. yallundae*.

Wild relatives of wheat, especially *Ae. tauschii*, have proven to be a rich reservoir of *R* genes, particularly against foliar pathogens such as rusts, powdery mildew and blast[21,26,32]. Many of these genes have been cloned using *k*-mer GWAS, an approach that leverages multiple reference genomes to identify presence/absence variants and structural polymorphisms not captured in single-reference analyses[21,26,33]. This strategy has proven particularly effective in highly diverse wild plant species, enabling identification and refinement of resistance-associated haplotypes even when structural variation complicates alignment to reference genomes. Despite its success for the study of foliar diseases, *Ae. tauschii* has remained underexplored for resistance to soil-borne diseases, including eyespot.

In this study, we identified *Pch4*, a novel NLR gene from *Ae. tauschii*, as a major source of resistance to *O. yallundae*. To our knowledge, *Pch4* represents the first cloned major *R* gene for eyespot resistance in cereals. Using *k*-mer GWAS on the *Ae. tauschii* L2 diversity panel, resistance was associated with a haplotype on chromosome 1DS containing two adjacent NLR genes. Of these, one showed a stronger correlation with the identified eyespot resistance, designated *Pch4*, and was investigated as the primary candidate. Transgenic expression of the *Pch4* candidate in the susceptible cultivar Chinese Spring confirmed that the gene confers robust, dominant resistance to *O. yallundae*, with a dosage-dependent effect observed in segregating populations.

Our phylogenetic analysis revealed that *Pch4* clusters with the well-characterized allelic series of powdery mildew resistance genes – *Pm3* (wheat), *Pm8* (rye), and *TmPm3* (*Triticum monococcum*) – all of which reside on the short arm of chromosome 1 in their respective species[29,30]. Synteny analysis supports a shared ancestral origin of *Pch4* and *Pm3* alleles, which is particularly interesting since *B. graminis* is an obligate oomycete pathogen while *O. yallundae* is facultative fungal pathogen with an extended viability in soils in the absence of living host tissue. Therefore, the evolutionary relationship of *Pch4* and *Pm3* alleles suggests that diversification of NLR gene families can yield resistance against ecologically and phylogenetically distinct pathogens.

A persistent challenge in deploying resistance from wild relatives is linkage drag, as well as regulatory hurdles associated with transgenic approaches in wheat[34]. Notably, *Pch4* was absent from a global panel of bread wheat landraces, indicating that this allele was not captured during wheat domestication and polyploidization, and underscoring the narrow genetic base of modern wheat[21]. Synthetic hexaploid wheats (SHWs), generated by crossing durum wheat with diverse *Ae. tauschii* accessions, provide a practical bridge for introducing such novel genes into breeding programs[21,35]. Genomic analysis of SHWs revealed that several lines carry *Pch4*, as well as multiple additional cloned *R* genes from *Ae. tauschii*, offering the potential for natural stacking of resistance loci. The increasing use of *Ae. tauschii* SHW in wheat breeding programs raises the tantalising possibility that this gene may already exist in elite backgrounds, free from undesirable linkage drag[27,36].

Although *Pch4* accounts for most observed resistance to eyespot in *Ae. tauschii* L2, subsets of resistant accessions in both L1 and L2 lack the gene, suggesting additional unexplored resistance sources. These may be revealed through complementary approaches such as positional cloning, mutational genomics, or GWAS analyses on an expanded diversity panel. Moreover, while *Pch4* specifically protects against *O. yallundae*, the potential for *Ae. tauschii* to harbour resistance against *O. acuformis* or other soil-borne pathogens remains unexplored and warrants further investigation.

Together, our results provide the first genetic insight into eyespot resistance from *Ae. tauschii* and establish *Pch4* as a deployable *R* gene for wheat breeding. The cloning of *Pch4* expands the limited arsenal of soil-borne resistance genes in cereals and highlights the evolutionary flexibility of NLR clusters in *Triticeae*. Looking forward, future work should focus on: (1) elucidating the molecular mechanism of *Pch4*-mediated recognition, (2) compare the structures of effectors from *O. yallundae* and *B. graminis* interacting with *Pch4* and *Pm3* alleles, respectively, to understand how this NLR gene family evolved to recognise distinct pathogens (3) surveying *Ae. tauschii* for additional soil-borne disease resistance genes, and (4) strategically combining *Pch4* with other *R* genes to enhance durability. These findings emphasize the untapped potential of wild relatives in safeguarding global wheat production.

Methods

Plant materials

The *Ae. tauschii* diversity panel germplasm and synthetic hexaploid wheat lines used in this study have previously been described and published[21,27]. The *Ae. tauschii* F_2 population was created by crossing accession BW_01185 with BW_01086 and advancing four F_1 progeny seed to F_2. Experimental control wheat cultivars with varying responses to eyespot were obtained from the John Innes Centre and RAGT. The *CS-Pch4* transgenic lines and all other germplasm used are detailed in Supplementary Table 14.

V8 agar plate preparation for the eyespot pathogens

To prepare 1 L of V8 agar, 200 ml of V8 juice (https://www.amazon.co.uk/V8-Vegetable-Juice-Original-1L/dp/B016OW5KZC), was combined with 800 ml sterile water and 15 g of agar. Solutions were autoclaved and allowed to cool sufficiently for handling, before dispensing into agar plates under sterile conditions.

O. yallundae and *O. acuformis* isolate collection and cultivation

O. yallundae isolate 20/848 was obtained from RAGT. This isolate was used for glasshouse phenotyping via dead oat inoculation. In brief, sterilised dead oats were inoculated with mycelium of isolate 20/848 and left to grow for several weeks until the mycelia were well developed. Oats were occasionally broken up by hand to increase inoculum mixing and speed up colonisation. Once visible mycelia could be seen ubiquitously throughout, the inoculum mix was ready for use. All other *Oculimacula* isolates were available at JIC (Supplementary Table 15). For growth room phenotyping, frozen agar mycelial stubs for all isolates were grown on V8 agar plates in the dark at 25°C for several weeks to bulk mycelia. If further inoculum was required, new plates were prepared using freshly cut mycelial stubs.

Isolates were subject to quality control via ITS sequencing, with a maximum likelihood phylogenetic tree built using PhyML 3.0[37] (500 bootstraps) to confirm that the correct species were used in this study (Supplementary Fig. 7). To extract DNA, cultures were grown from a single mycelium plug in 10 ml of Potato Dextrose Broth (Formedium, UK). After 7 days, cultures were centrifuged, the supernatant removed, and ~ 250 mg of mycelial pellet was crushed in liquid nitrogen with pestle and mortar or with glass beads in a TissueLyser II (Qiagen, Germany). The disrupted tissue was then integrated into the workflow for the soil gDNA extraction kit, DNeasy® PowerSoil® Pro (Qiagen, Germany), following the manufacturer's instructions. DNA quality and concentration were evaluated by Nanodrop and Qubit. ITS sequencing via PCR was carried out using primers TCCTCCGCTTATTGATATGC and GGAAGTAAAAGTCGTAACAAGG, with PCR products purified using the Machery-Nagel NucleoSpin kit (ID: 740609.50)[38]. ITS sequences were sequenced using Sanger sequencing by Eurofins.

Ae. tauschii eyespot disease scale development

Disease scoring utilised a modified version of an existing protocol[22]. For each biological replicate, the plant was uprooted, and cleaned to remove as much soil as possible, then given a disease severity score based upon the layers of sheath infected or penetrated; 0 = no infection detected, 1 = coleoptile infected, 2 = coleoptile penetrated, 3 = first sheath infected, etc. A score of 9 was determined to be the highest using this scale as plants observed with this level of disease represented near total infection of the entire stem, with individual layers of plant sheath nearly impossible to identify due to the deteriorated state of the diseased tissue.

Glasshouse phenotyping

Disease responses were assessed for the *Ae. tauschii* L2 diversity panel via a seedling bioassay in unheated, unlit, glasshouses in Cambridge from November 2022 to February 2023. Four seeds of each

accession in addition to control wheat varieties were sown in three replicated trials by placing seed in rows atop compost. Seeds were inoculated with *O. yallundae* isolate 20/848 by applying a mixture of infected dead oats through which seedlings would grow, using an established method[39]. Plants were regularly watered to ensure a moist damp environment optimal for pathogen infection, with the plants deemed ready for phenotyping once the susceptible control wheat lines had reached a phenotype score of 9. Each plant was individually uprooted and washed to remove residual soil before phenotypic assessment.

Growth room phenotyping

Controlled environment rooms were used for all other phenotyping assays, including the *Ae. tauschii* L1 diversity panel, SHW and transgenic lines. Plants were grown at 10°C under a 10h day / 14h night cycle in JIC cereal mix and inoculated using an established method[40]. Briefly, seeds were sown in 96 well trays of JIC cereal mix, watered and allowed to germinate. At about 5–7 days of growth, ~ 1-inch-long PVC cylinders were placed over emerging plant shoots and slightly embedded in the soil to maintain their upright position. Once plants had reached a two-leaf growth stage, typically two weeks post seedling emergence, plants were individually inoculated with *O. yallundae* or *O. acuformis* via a pathogen containing agar slurry. This agar slurry was prepared using colonies of *Oculimacula* species grown on V8 media agar plates that were homogenised with water in a 2:1 ratio using a hand blender. A sterile syringe was used to fill the PVC cylinder surrounding each seedling until the entire stem base was in contact with the pathogen. Plants were watered thoroughly from the bottom of the tray and covered for the first 48 hours to increase humidity before being left to grow at 10°C under a 10h day / 14h night light cycle for 10 weeks, with scoring date determined by the level of disease severity in the susceptible wheat control line, Chinese Spring.

k-mer based GWAS

k-mer based GWAS was performed based on an established method[21] using the reference genome assembly TA1675[23]. For isolate 20/848 the phenotypic scores of each accession in the *Ae. tauschii* L2 diversity panel were averaged across the three replicated trials and inverted so that a lower value represents a more susceptible accession. Values deemed intermediate (between − 5.51 and − 7.5) were removed to produce a dataset of clearly susceptible and clearly resistant accessions. A negative log *p*-value significance threshold of 9.3, estimated previously[21], was applied.

Pch4 Kompetitive Allele-specific PCR markers development

The *Pch4* nucleotide sequence of resistant and susceptible alleles in lines BW_01185 and BW_01086 was aligned in Geneious to identify regions suitable for the design of KASP markers capable of differentiating between them. The markers were used to genotype the BW_01185 x BW_01086 F_2 population. To create markers capable of differentiating the alleles in a hexaploid wheat background, *Pch4* was aligned to the wheat assembly Robigus,

(https://ensembl.gramene.org/Triticum_aestivum_robigus/Info/Index) using BLASTn[24] to extract the A, B and D genome homoeologs. Alignment of these nucleotide sequences identified a region suitable to create KASP markers where both the common and differentiating markers were specific to the D genome. The homoeolog specific markers were validated using a SHW-BC F_5 population, NIAB-SHW-BC-219 (SHW-069 x Robigus). All KASP assays were set up using PACE® genotyping master mix, according to the manufacturer's instructions (https://3crbio.com/products/), and run using a standard touchdown PCR programme; 94°C for 15 minutes, 94°C for 20 seconds, 65°C for 1 minute (repeated x10, with temperature decreasing by 0.8°C each cycle to 57°C), 94°C for 20 seconds followed by 57°C for 1 minute (repeated x35). Additional cycles were added as required to achieve maximum separation between different genotypes. Plates were read using a PHERAstar microplate and analysed using KlusterCaller software.

Fungal infection microscopy

The fungal chitin visualisation technique was adapted from an existing protocol[41]. Tissue from the hypocotyl region of each plant was cut into lengths of ~ 5 mm length and embedded in 1.5 ml Eppendorf tubes filled with 7% low melting point agarose and set at 4°C for 2–4 hours. Embedded samples were sectioned using a VT1000 vibratome to a thickness of 200 µm and transferred onto microscope slides using forceps and cotton-buds. To visualise fungal chitin, samples were stained with Invitrogen Wheat Germ Agglutinin Alexa Fluor® 488 conjugate (WGA-AF-488) (50 mg/mL) for 20 minutes. Stained sections were washed twice with PBS to minimise background staining. Microscopic analysis was performed on a Zeiss Axio Zoom V16 microscope with a 1.0x/0.25 air objective. Using the Spectra 3 Light Engine, a cyan laser at 100% intensity was filtered through a 38 HE GFP (Alexa 488/GFP) filter block. To obtain higher contrast images, a ZEISS Apotome 3 was utilized for optical sectioning in GFP channels. Image acquisition and processing was performed with the Zeiss ZenBlue microscopy software (www.zeiss.com) through both monochrome and colour cameras with an exposure time of 200 ms.

Pch4 gene cloning, domestication and transformation

Fresh genomic DNA of *Ae. tauschii* accession BW_01016 was extracted from young leaf tissue using the Qiagen Plant DNeasy minikit (ID: 69104). The publicly available genome annotation for the *Ae. tauschii* reference assembly TA1675 was used to predict the start and stop codon for *Pch4*, and the primers ES_GG_F and ES_GG_R (Supplementary Table 10) were designed 1kb up and downstream of the gene start and stop codons, respectively. Phusion polymerase (New England Biolabs (NEB), ID: M0530S) was used to amplify the target product using standard PCR amplified as per the manufacturer's instructions (Tm60, 35x cycles). Briefly, a 100µ reaction was set up using DNA from BW_01016 as the template and amplified as per manufacturer's instructions. The PCR product size was confirmed using a 1% agarose and ethidium bromide gel to confirm the target band size under UV light, before the product was excised and cleaned using a Machery-Nagel NucleoSpin kit (ID: 740609.50) A poly-A overhang was introduced onto the 3' ends of the linear PCR product using Q5® High-Fidelity DNA Polymerase (Neb, ID: M0491S) before ligation into a pGEM®-T Easy Vector (Promega), according to the manufacturer's instructions.

The ligated vector was transformed into JM109 competent cells (Promega) using heat shock and screened via blue-white selection for successful transformants. A colony PCR was used to confirm the presence of the genomic *Pch4* sequence in a colony using primer pair ES_GG_F and ES_GG_R, and correctly cloned transformants confirmed using nanopore sequencing from Plasmidsaurus (https://www.plasmidsaurus.com).

To produce a gene construct amenable to golden gate assembly, four BpiI and one BsaI enzyme cut sites were domesticated by taking advantage of redundancies in the genetic code. In short, a suite of primers (ES_dom_1_F to ES_dom_12_R, Supplementary Table 10) with overhanging BpiI sites that enabled one directional seamless ligations was used to amplify five individual PCR products with single bp changes in the primer sequences that targeted each enzyme cut site. The pGEM-*Pch4* plasmid was used as the template for fragment amplification, using the same PCR conditions as above. All DNA fragments were confirmed by visualisation on an agarose gel before gel excision and product clean up using the NucleoSpin kit. Fragments were assembled via BpiI golden gate assembly[42] directly into a level 0 vector pICH41308 (Addgene #47998). Successful domestication was confirmed via Plasmidsaurus whole plasmid sequencing. The golden gate assembly protocol was followed using restriction enzyme BsaI to combine a Rice actin 1 promotor with 5' UTR (OsAct1) pICSL12014 (Addgene #125882), the *Pch4* gDNA, and a 35S terminator with 3' UTR pICH41414 (Addgene # 50337), into a level 1 position 3 vector (L1P3) pICH47822 (Addgene #48009).

The L1P3 *Pch4* plasmid was transferred to the JIC wheat transformation team, where it was assembled along with the Level 1 hygromycin selectable marker gene (Addgene # 165423) into the wheat transformation binary vector pGoldenGreenGate-M (pGGG-M) (Addgene # 165422) as previously described[43]. Wheat transformation was carried out following an established method[44], resulting in two successful transformed T_0 plants with either one or six copies of the *Pch4* transgene. Transformants and null controls were advanced to T_1 and T_2 for phenotyping. Gene copy number quantification was performed for the T_0 and T_1 plants by the JIC in house genotyping platform, using the hygromycin resistance gene that is introduced into wheat as a selectable marker alongside *Pch4* for qRT-PCR and the previously outlined methodology[45].

NLR phylogenetics

NLR genes and their corresponding NBARC domains from the *Ae. tauschii* reference genome TA1675 were identified using NLR-Annotator[46]. These sequences were concatenated with those from the RefPlantNLR dataset[28] and aligned using Clustal Omega[47]. Phylogenetic inference was performed with RAxML v8.2.12[48] using the Maximum Likelihood method under the JTT substitution model (command: raxmlHPC-PTHREADS-AVX2 -T 10 -s Pch4_clustal_allignment_070124.phy -n RefPlantNLR -m PROTGAMMAAUTO -f a -# 1000 -x 8153044963028367 -p 644124967711489). The resulting phylogenetic tree was visualized and edited using the iTOL suite[49].

Synteny analysis

To investigate gene collinearity and identify orthologous relationships among grass genomes, the JCVI utility library was employed (https://github.com/tanghaibao/jcvi) to perform pairwise orthology detection and synteny screening. Analyses were conducted between the following genome pairs in progressive evolutionary order: *Brachypodium distachyon* vs. *Hordeum vulgare*, *Hordeum vulgare* vs. *Secale cereale*, *Secale cereale* vs. *T. monococcum, T. monococcum* vs. *T. aestivum* A genome, *T. aestivum* A vs. B genomes, *T. aestivum* B vs. D genomes, *T. aestivum* D genome vs. *Aegilops tauschii.* The reference genomes used are detailed in Supplementary Table 16. For synteny analysis, gene annotation files were converted into .bed format using the JCVI suite. For each file, the following steps were executed: The .gff3.gz files were decompressed using gunzip. Each .gff3 file was converted to BED format using the jcvi.formats.gff module of the JCVI utility suite. Specifically, the bed subcommand was used with the options --type = gene and --key = ID to extract gene features based on their unique identifiers. Files containing the coding sequences were modified using awk and sed commands so that gene names matched with the .bed files and all transcripts except the first were removed.

For each genome pair, orthologs were identified using the jcvi.compara.catalog ortholog module with the --no_strip_names option to preserve original gene identifiers. Anchor files generated from this step were then refined using the jcvi.compara.synteny screen command to retain syntenic blocks with a minimum span of 30 genes and using the --simple flag for simplified filtering. Microsyteny was plotted using the jcvi.graphics.synteny module where the gene **Aet.TA1675.r1.1D001090** was highlighted in green, while **Aet.TA1675.r1.1D001100 and Aet.TA1675.r1.1D001300** were highlighted in orange (see Fig. 4c).

Cloned *R* gene prediction in *Ae. tauschii* L2 diversity panel

The nucleotide sequences for cloned *Ae. tauschii R* genes (except where indicated below) were obtained from online data repositories (Supplementary Table 17). Each gene was used as the input query to search the available contig level whole-genome assemblies[21] and RenSeq assemblies[32] of the L2 diversity panel using BLASTn[24]. An *R* gene was determined to be present within an accession if the majority of the gene could be identified from the BLASTn[24] results with a percentage identity relative to the query of 99.5%. In multiple cases *R* genes were present across numerous contigs, requiring significant manual curation and care in order to determine *R* gene presence. For *Stb16q* and *Lr39*, the *R* gene linked KASP markers reported in the literature[23,50] were used as the input query for search using BLASTn-short[24]. For *Sr66 (SrTA1662), Sr33, Sr45, Sr46, Cmc4* and *WTK4* genes, their presence within the panel had already been reported in previous studies[21,32]. The phylogenetic tree and gene presence was plotted in iToL, with colours added to distinguish associated disease resistance.

Declarations

Acknowledgements

This work was supported by a John Innes Foundation fellowship to SA and by UKRI BBSRC through the Institute Strategic Programme grant BB/X010996/1 (Advancing Plant Health) and BB/P012574 (Plant

Health). DG was supported by a BBSRC/RAGT Industrial-Collaborative Award in Science and Engineering fellowship. PN was supported by UKRI BBSRC through the Institute Strategic Programme grant BB/P016855/1 (Designing Future Wheat) and BB/X011003/1 (Delivering Sustainable Wheat). We are grateful to Kara Boyd (JIC) for assistance with plant husbandry work, and to Claire Domoney (JIC) and Mark Banfield (JIC) for reviewing the draft manuscript. The high-performance computing resources and services used in this work were supported by the Norwich Bioscience Institutes Partnership (NBIP) Computing infrastructure for Science (CiS) group. We are grateful to the John Innes Centre (JIC) Horticultural Services for plant greenhouse support and R. Goram at the JIC genotyping platform for genotyping support. We also thank RAGT Seeds for providing access to their greenhouses and resources for conducting the phenotyping work and thank Chris Burt for his constructive feedback. Lastly, we thank NIAB for providing us with seed of the synthetic hexaploid wheat backcross population, NIAB-SHW-BC-219.

Contributions

S.A. designed the research; D.G. and K.G. performed *k*-mer-based GWAS and refined the resistance mapping interval; D.G., A.P., C.M., R.B. conducted phenotyping of the diversity panel, and synthetic and transgenic wheat; P.N., A.S. and T.H., provided *Oculimacula* isolates and plant phenotyping support; D.G. designed the binary construct; S.H. and M.S. carried out wheat transformation; D.G. performed KASP marker analysis; N.T. conducted microscopic analysis; A.P.M and S.B. cultured *Oculimacula* isolates for sequencing to build the phylogenetic tree; R.M. generated the *Ae. tauschii* F_2 population; D.G., K.G. and S.A. drafted the manuscript; D.G., K.G., M.V. and S.A. designed the figures; All authors reviewed and approved the manuscript.

Ethics declarations

Competing interests

The authors declare no competing interests.

References

1. Crous PW, Groenewald JZE, Gams W (2003) Eyespot of cereals revisited: ITS phylogeny reveals new species relationships. Eur J Plant Pathol 109:841–850. 10.1023/A:1026111030426
2. Burt C, Hollins TW, Powell N, Nicholson P (2010) Differential seedling resistance to the eyespot pathogens, *Oculimacula yallundae* and *Oculimacula acuformis*, conferred by *Pch2* in wheat and among accessions of *Triticum monococcum*. Plant Pathol 59:819–828. 10.1111/j.1365-3059.2010.02307.x
3. Ray RV, Crook MJ, Jenkinson P, Edwards SG (2006) Effect of eyespot caused by *Oculimacula yallundae* and *O. acuformis*, assessed visually and by competitive PCR, on stem strength associated

with lodging resistance and yield of winter wheat. Journal Experimental Botany 57:2249–2257. 10.1093/jxb/erj192

4. Meyer N et al (2011) Diagnostic value of molecular markers linked to the eyespot resistance gene *Pch1* in wheat. Euphytica 177:267–275. 10.1007/s10681-010-0266-0
5. Parnell S, Gilligan CA, Lucas JA, Bock CH, Van Den Bosch F (2008) Changes in fungicide sensitivity and relative species abundance in *Oculimacula yallundae* and *O. acuformi*s populations (eyespot disease of cereals) in Western Europe. Plant Pathol 57:509–517. 10.1111/j.1365-3059.2007.01786.x
6. Hollins TW, Scott PR, Paine JR (1985) Morphology, benomyl resistance and pathogenicity to wheat and rye of isolates of *Pseudocercosporella herpotrichoides*. Plant Pathol 34:369–379. 10.1111/j.1365-3059.1985.tb01375.x
7. Cadle MM, Murray TD, Jones SS (1997) Identification of resistance to *Pseudocercosporella herpotrichoides* in *Triticum monococcum*. Plant Dis 81:1181–1186. 10.1094/PDIS.1997.81.10.1181
8. Sheng H, Murray TD (2013) Identifying new sources of resistance to eyespot of wheat in *Aegilops longissima*. Plant Dis 97:346–353. 10.1094/PDIS-12-11-1048-RE
9. Worland AJ, Law CN, Hollins TW, Koebner RMD, Giura A (1988) Location of a gene for resistance to eyespot (P*seudocercosparella herpotrichoides*) on chromosome 7D of bread wheat. Plant Breeding 101:43–51. 10.1111/j.1439-0523.1988.tb00265.x
10. de la Pena RC, Murray TD, Jones SS (1996) Linkage relations among eyespot resistance gene *Pch2*, endopeptidase Ep–A1b, and RFLP marker Xpsr121 on chromosome 7A of wheat. Plant Breeding 115:273–275. 10.1111/j.1439-0523.1996.tb00916.x
11. Murray TD, de la Pena RC, Yildirim A, Jones SS, Qualset CO (1994) A new source of resistance to *Pseudocercosporella herpotrichoides*, cause of eyespot disease of wheat, located on chromosome 4V of *Dasypyrum villosum*. Plant Breeding 113:281–286. 10.1111/j.1439-0523.1994.tb00737.x
12. Muranty H, Jahier J, Tanguy A–M, Worland AJ, Law C (2002) Inheritance of resistance of wheat to eyespot at the adult stage. Plant Breeding 121:536–538. 10.1046/j.1439-0523.2002.00767.x
13. Burt C, Hollins TW, Nicholson P (2011) Identification of a QTL conferring seedling and adult plant resistance to eyespot on chromosome 5A of Cappelle Desprez. Theor Appl Genet 122:119–128. 10.1007/s00122-010-1427-1
14. Pasquariello M, Berry S, Burt C, Uauy C, Nicholson P (2020) Yield reduction historically associated with the *Aegilops ventricosa* 7DV introgression is genetically and physically distinct from the eyespot resistance gene *Pch1*. *Theoretical and Applied Genetics* 133, 707–717 10.1007/s00122-019-03502-1
15. Zanke CD et al (2017) Genome–wide association mapping of resistance to eyespot disease (P*seudocercosporella herpotrichoides*) in European winter wheat (*Triticum aestivum* L.) and fine–mapping of *Pch1*. Theor Appl Genet 130:505–514. 10.1007/s00122-016-2830-z
16. Lewien MJ, Murray TD, Jernigan KL, Garland–Campbell KA, Carter AH (2018) Genome–wide association mapping for eyespot disease in US Pacific Northwest winter wheat. PLoS ONE

13:e0194698. 10.1371/journal.pone.0194698

17. Burt C et al (2014) Mining the Watkins collection of wheat landraces for novel sources of eyespot resistance. Plant Pathol 63:1241–1250. 10.1111/ppa.12221
18. Thiele A, Schumann E, Peil A, Weber WE (2008) Eyespot resistance in wheat × *Aegilops kotschyi* backcross lines. Plant Breeding 121:29–35. 10.1046/j.1439-0523.2002.00669.x
19. Yildirim A, Jones SS, Murray TD, Cox TS, Line RF (1995) Resistance to stripe rust and eyespot diseases of wheat in *Triticum tauschii*. Plant Dis 79:1230–1236. 10.1094/PD-79-1230
20. Hafeez AN et al (2021) Creation and judicious application of a wheat resistance gene atlas. Mol Plant 14:1053–1070. 10.1016/j.molp.2021.05.014
21. Gaurav K et al (2022) Population genomic analysis of *Aegilops tauschii* identifies targets for bread wheat improvement. Nat Biotechnol 40:422–431. 10.1038/s41587-021-01058-4
22. Scott PR (1971) The effect of temperature on eyespot (*Cercosporella herpotrichoides*) in wheat seedlings. Ann Appl Biol 68:169–175. 10.1111/j.1744-7348.1971.tb06453.x
23. Cavalet–Giorsa E et al (2024) Origin and evolution of the bread wheat D genome. Nature 633:848–855. 10.1038/s41586-024-07808-z
24. Camacho C et al (2009) BLAST+: architecture and applications. BMC Bioinformatics 10:421. 10.1186/1471-2105-10-421
25. Blum M et al (2021) The InterPro protein families and domains database: 20 years on. Nucleic Acids Res 49:D344–D354. 10.1093/nar/gkaa977
26. Arora S et al (2023) A wheat kinase and immune receptor form host-specificity barriers against the blast fungus. Nat Plants 9:385–392. 10.1038/s41477-023-01357-5
27. Wright TIC et al (2024) A new winter wheat genetic resource harbors untapped diversity from synthetic hexaploid wheat. Theor Appl Genet 137:73. 10.1007/s00122-024-04577-1
28. Kourelis J, Sakai T, Adachi H, Kamoun S (2021) RefPlantNLR is a comprehensive collection of experimentally validated plant disease resistance proteins from the NLR family. PLoS Biol 19:e3001124. 10.1371/journal.pbio.3001124
29. Hurni S et al (2013) Rye *Pm8* and wheat *Pm3* are orthologous genes and show evolutionary conservation of resistance function against powdery mildew. Plant J 76:957–969. 10.1111/tpj.12345
30. Zhao CZ et al (2016) Molecular cloning, functional verification, and evolution of *TmPm3*, the powdery mildew resistance gene of *Triticum monococcum* L. Genet Mol Res 15(2). 10.4238/gmr.15028056
31. Burt C, Nicholson P (2011) Exploiting co-linearity among grass species to map the *Aegilops ventricosa*-derived *Pch1* eyespot resistance in wheat and establish its relationship to *Pch2*. *Theor. Appl. Genet.* 123, 1387–1400 10.1007/s00122-011-1674-9
32. Arora S et al (2019) Resistance gene cloning from a wild crop relative by sequence capture and association genetics. Nat Biotechnol 37:139–143. 10.1038/s41587-018-0007-9

33. Voichek Y, Weigel D (2020) Identifying genetic variants underlying phenotypic variation in plants without complete genomes. Nat Genet 52:534–540. 10.1038/s41588-020-0612-7
34. Rafiei F et al (2024) Facts, uncertainties, and opportunities in wheat molecular improvement. Heredity 133:371–380. 10.1038/s41437-024-00721-1
35. Ogbonnaya FC et al (2013) Synthetic Hexaploids: Harnessing Species of the Primary Gene Pool for Wheat Improvement. Plant Breeding Reviews, vol 37. Janick J., editor; Wiley-Blackwell, Hoboken, NJ, pp 35–122
36. Rosyara U et al (2019) Genetic Contribution of Synthetic Hexaploid Wheat to CIMMYT's Spring Bread Wheat Breeding Germplasm. Sci Rep 9:12355. 10.1038/s41598-019-47936-5
37. Guindon S et al (2010) New Algorithms and Methods to Estimate Maximum-Likelihood Phylogenies: Assessing the Performance of PhyML 3.0. Syst Biol 59:307–321. 10.1093/sysbio/syq010
38. White TJ, Bruns TD, Lee SB, Taylor JW (1990) Amplification and direct sequencing of fungal ribosomal RNA genes for phylogenetics. In *PCR Protocols: A Guide to Methods and Applications*, Innis M. A., Gelfand D. H., Sninsky J. J. & White T. J., eds.; Academic Press: New York, 315–322 10.1016/B978-0-12-372180-8.50042-1
39. Bruehl GW, Nelson WL (1964) Technique for mass inoculations of winter wheat in the field with *Cercosporella herpotrichoides*. FJ Dis Reptr 48:863–865. https://www.cabidigitallibrary.org/doi/full/10.5555/19651101053
40. Chapman NH, Burt C, Nicholson P (2009) The identification of candidate genes associated with *Pch2* eyespot resistance in wheat using cDNA-AFLP. Theor Appl Genet 118:1045–1057. 10.1007/s00122-009-0961-1
41. Djébali N, Jauneau A, Ameline-Torregrosa C, Chardon F, Jaulneau V, Mathé C, Bottin A, Cazaux M, Pilet-Nayel M-L, Baranger A, Aouani ME (2009) Partial resistance of *Medicago truncatula* to *Aphanomyces euteiches* is associated with protection of the root stele and is controlled by a major QTL rich in proteasome-related genes. Mol Plant-Microbe Interact 22:1043–1055. 10.1094/MPMI-22-9-1043
42. Weber E, Engler C, Gruetzner R, Werner S, Marillonnet S (2011) A Modular Cloning System for Standardized Assembly of Multigene Constructs. PLoS ONE 6:e16765. 10.1371/journal.pone.0016765
43. Smedley MA, Hayta S, Clarke M, Harwood WA (2021) CRISPR-Cas9 Based Genome Editing in Wheat. Curr Protoc 1:e65. 10.1002/cpz1.65
44. Hayta S, Smedley MA, Clarke M, Forner M, Harwood WA (2021) An efficient Agrobacterium-mediated transformation protocol for hexaploid and tetraploid wheat. Curr Protoc 1:e58. 10.1002/cpz1.58
45. Hayta S, Smedley MA, Demir SU et al (2019) An efficient and reproducible *Agrobacterium*-mediated transformation method for hexaploid wheat (*Triticum aestivum* L). Plant Methods 15:121. 10.1186/s13007-019-0503-z
46. Steuernagel B et al (2020) The NLR-Annotator tool enables annotation of the intracellular immune receptor repertoire. Plant Physiol 183:468–482. 10.1104/pp.19.01273

47. Sievers F et al (2011) Fast, scalable generation of high-quality protein multiple sequence alignments using Clustal Omega. Mol Syst Biol 7:539. 10.1038/msb.2011.75
48. Stamatakis A (2014) RAxML version 8: a tool for phylogenetic analysis and post-analysis of large phylogenies. Bioinformatics 30:1312–1313. 10.1093/bioinformatics/btu033
49. Letunic I, Bork P (2024) Interactive Tree of Life (iTOL) v6: recent updates to the phylogenetic tree display and annotation tool. Nucleic Acids Res 52:W78–W82. 10.1093/nar/gkae268
50. Saintenac C et al (2021) A wheat cysteine-rich receptor-like kinase confers broad-spectrum resistance against *Septoria tritici* blotch. Nat Commun 12:433. 10.1038/s41467-020-20685-0

Figures

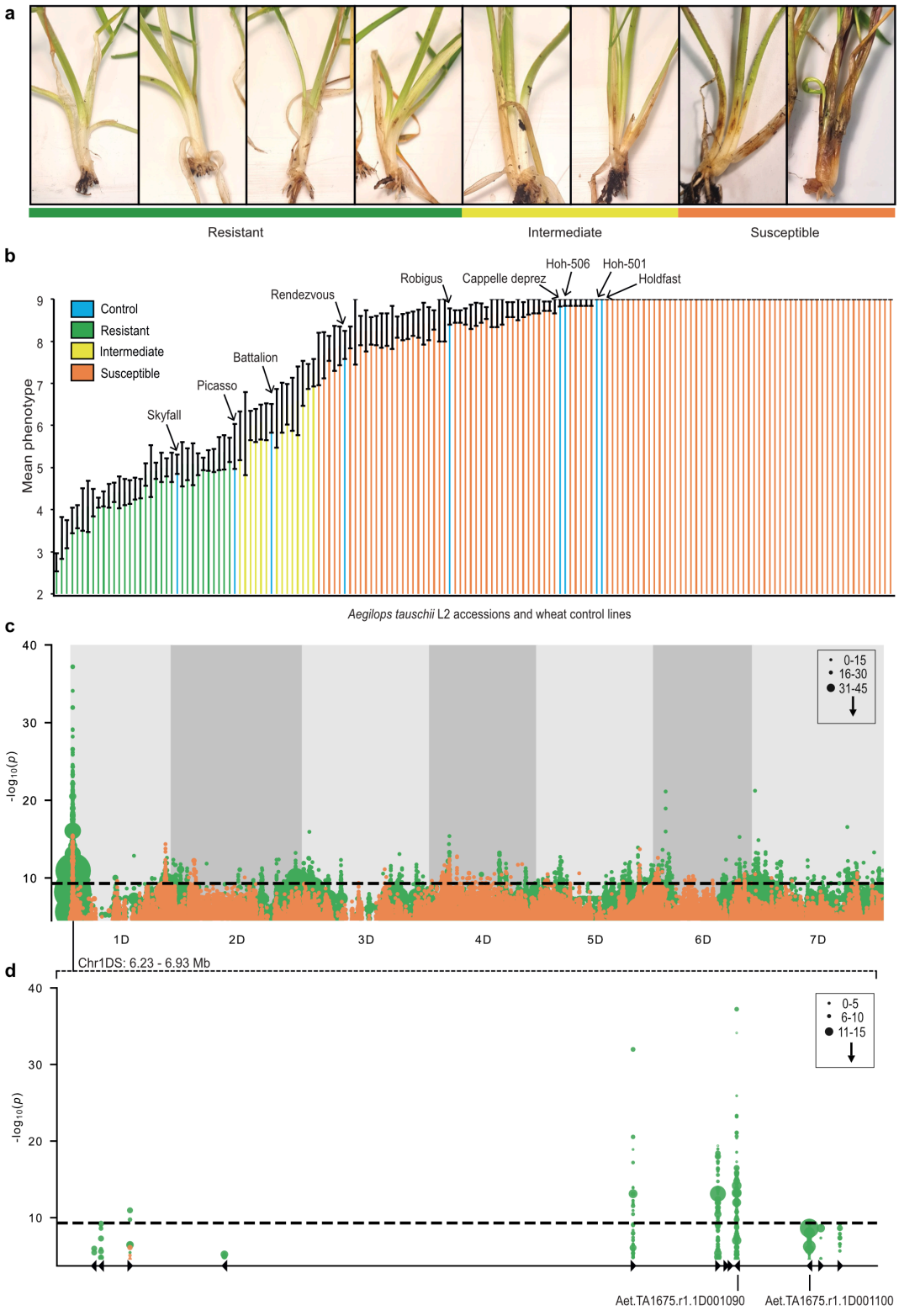

Figure 1

Identification of a novel eyespot resistance interval. a, *Ae. tauschii* specific phenotyping scale for eyespot disease severity. **b,** Phenotypic mean (n = 12) for the *Ae. tauschii* L2 panel (in green, amber and orange) and wheat control varieties (blue). **c,** Manhattan plot of the *k*-mer GWAS for eyespot disease resistance. The size of dots is proportional to the number of *k*-mers having a specific negative log *p*-value and their colour indicates a positive (green) or negative (orange) correlation with the phenotype. A

0.7 Mb interval on Chr 1D shows a significant positive association with eyespot resistance. **d,** Zooming-in on the associated 0.7 Mb interval on Chr 1D reveals 12 genes (black triangles), including two NLRs**,** ***Aet.TA1675.r1.1D001090*** and ***Aet.TA1675.r1.1D001100*****,** highlighted in the figure, with the most significant *k*-mers mapping to the former of the two.

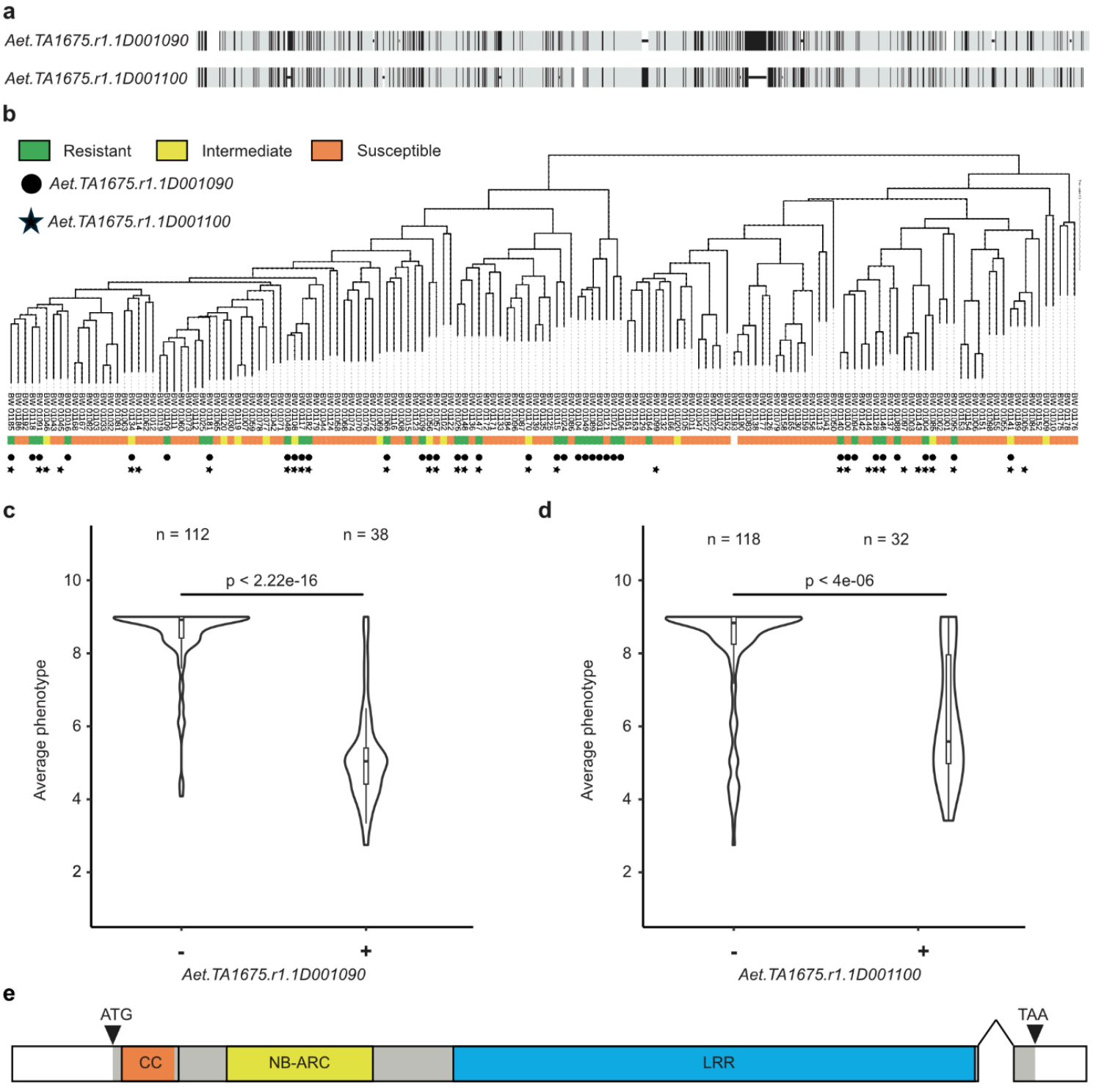

Figure 2

Differentiating the two NLRs in *Pch4* resistance interval and prioritising one for functional validation. a, MAFFT alignment of the two NLR candidate genes showed a pairwise nucleotide identity of 82.9% with

dissimilarities indicated by black lines **b,** Phylogenetic tree of *Ae. tauschii* L2 accessions with the mean eyespot disease phenotype and the presence of ***Aet.TA1675.r1.1D001090*** and ***Aet.TA1675.r1.1D001100*** indicated by the coloured boxes, black dots and black stars respectively. **c, *Aet.TA1675.r1.1D001090*** is present in 38 accessions with significantly reduced disease phenotype score (median average phenotype = 5.04) compared to the 112 accessions having alternate alleles (median average phenotype = 8.92; Mann-Whitney U, $p < 2.22x10^{-16}$). **d, *Aet.TA1675.r1.1D001100*** shows a significant (Mann-Whitney U, $p < 4x10^{-6}$) but reduced association with eyespot resistance compared to ***Aet.TA1675.r1.1D001090***. **e, *Aet.TA1675.r1.1D001090***, the primary *Pch4* candidate, encodes a two-exon canonical NLR**.**

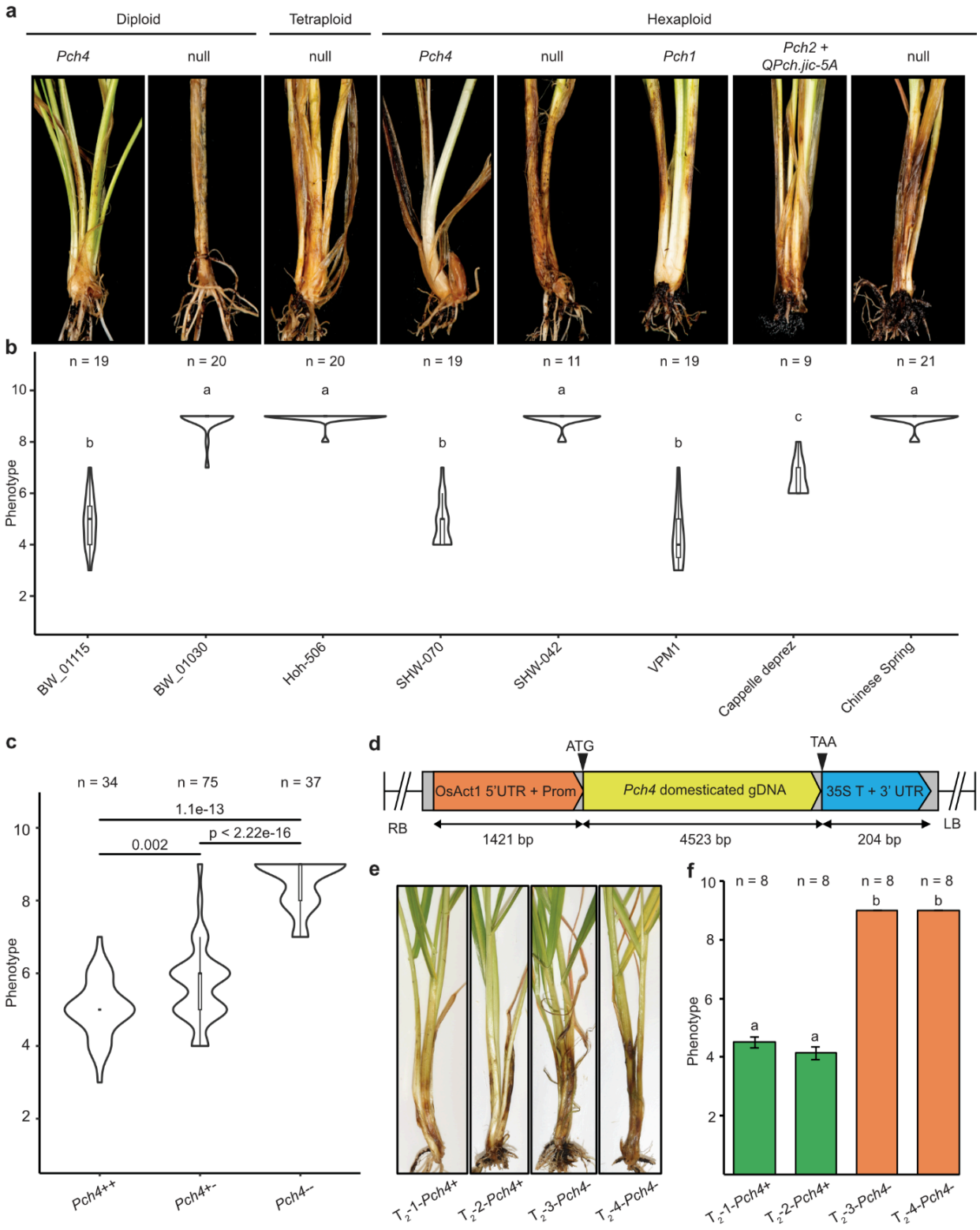

Figure 3

***Pch4* confers eyespot resistance in hexaploid wheat and exhibits a dosage dependent effect. a,** Representative phenotyping of resistant and susceptible diploid D genome donors, tetraploid parent and hexaploid synthetic and control lines. **b,** *Pch4* resistance in a synthetic hexaploid background confers a similar level of protection against *O. yallundae* as *Pch1.* Pairwise comparisons were performed using Wilcoxon rank-sum tests with Benjamini-Hochberg correction for multiple testing. Significant differences

were found between accessions containing *Pch4* (BW_01115, median = 5; SHW-070, median = 5), or VPM1 (containing *Pch1*, median = 4) compared to Cappelle Desprez (containing *Pch2* and QPch.jic-5A, median = 6) or accessions lacking any known eyespot resistance (BW_01030, median = 9; Hoh-506, median = 9; SHW-042, median = 9). **c,** Phenotyping of a biparental F_2 population derived from the BW_01185 x BW_01086 cross shows that *Pch4* acts as a dosage dependent dominant gene with a single copy significantly reducing disease phenotype. A Kruskal-Wallis rank sum test was conducted to determine differences in phenotype scores among the three genotypes *Pch4* ++ (median= 5, n = 34), *Pch4* +- (median = 6, n = 75), and Pch4 -- (median = 9, n = 37), showing statistically significant differences between the groups ($H(2) = 85.02$, $p < 0.001$). Post-hoc pairwise comparisons were performed using Wilcoxon rank-sum tests with Benjamini-Hochberg correction for multiple testing. Significant differences were found between genotypes Pch4 ++ and *Pch4* +- ($p = 0.002$), *Pch4* +- and *Pch4* -- ($p < 0.001$), and *Pch4* ++ and *Pch4* -- ($p < 0.001$). **d,** *Pch4* transgenic expression cassette containing the *OsAtct1* promoter and 5'UTR, domesticated *Pch4* genomic sequence and 35S terminator and 3'UTR (not drawn to scale). **e,** Disease infection assays of T_2 sister lines show appreciable differences in disease severity depending on the presence or absence of *Pch4.* **f,** Bar chart of T_2 sister lines (n = 8), pairwise comparisons were performed using Wilcoxon rank-sum tests with Benjamini-Hochberg correction for multiple testing. Significant differences were found for the comparison between *Pch4* containing transgenic cultivars (T_2-1-*Pch4+*, median = 4.5; T_2-2-*Pch4+*, median = 4) and transgenic nulls lacking *Pch4* (T_2-3-*Pch4-*, median = 9; T_2-4-*Pch4-,* median = 9; $p < 0.001$).

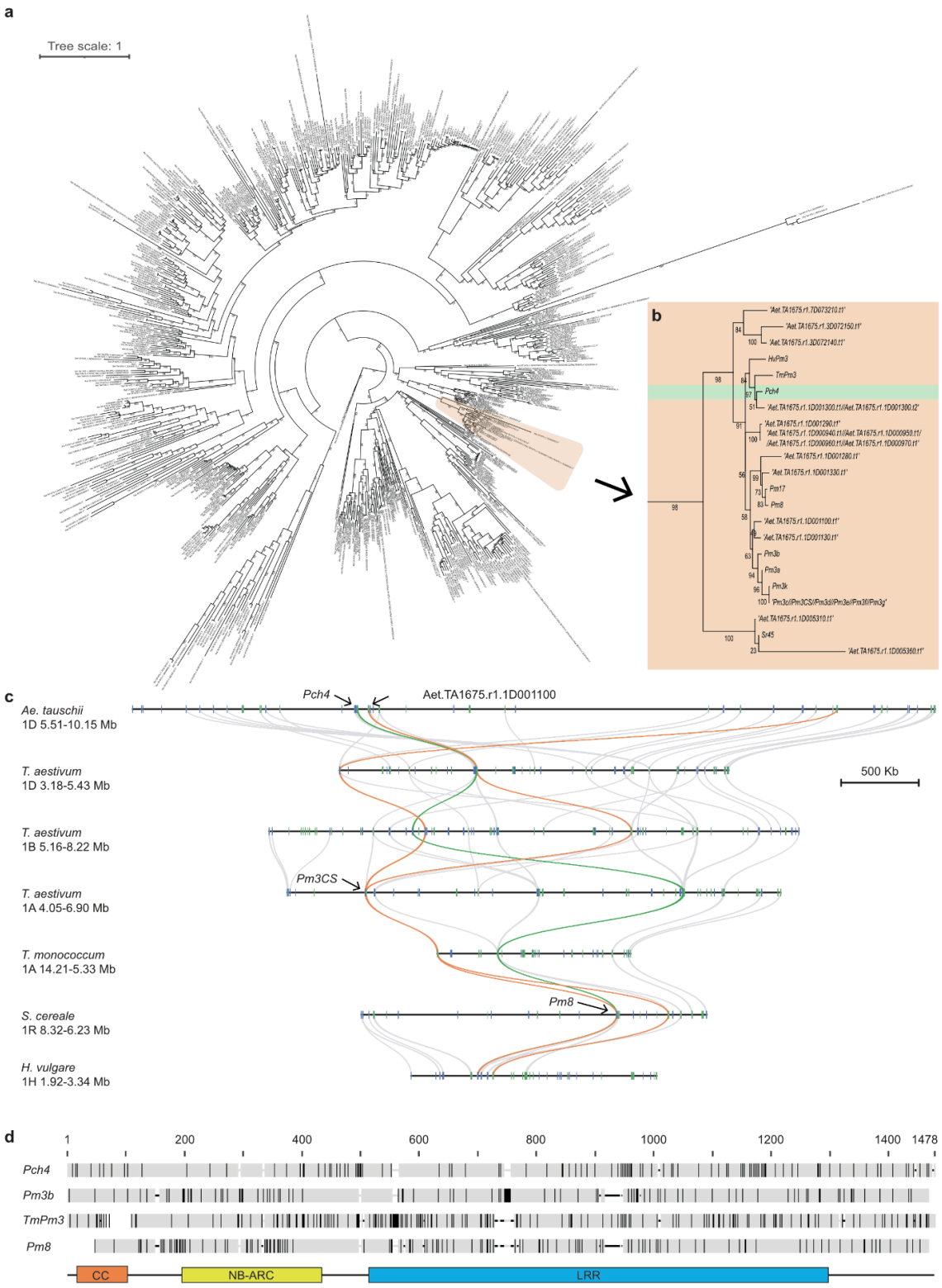

Figure 4

***Pch4*belongs to the same NLR lineage as *Pm3.* a,** Phylogenetic tree of NLRs extracted from TA1675 and RefPlantNLR. **b**, Zoom-in of phylogenetic clade containing *Pch4* and *Pm3* orthologs. **c**, Microsynteny plot of orthologous regions in *Ae. tauschii*, *T. aestivum, T. monococcum, S. cereale* and *H. vulgare.* **d,** MAFFT alignment of the amino acid sequences of *Pch4, TmPm3, Pm3b* and *Pm8.*

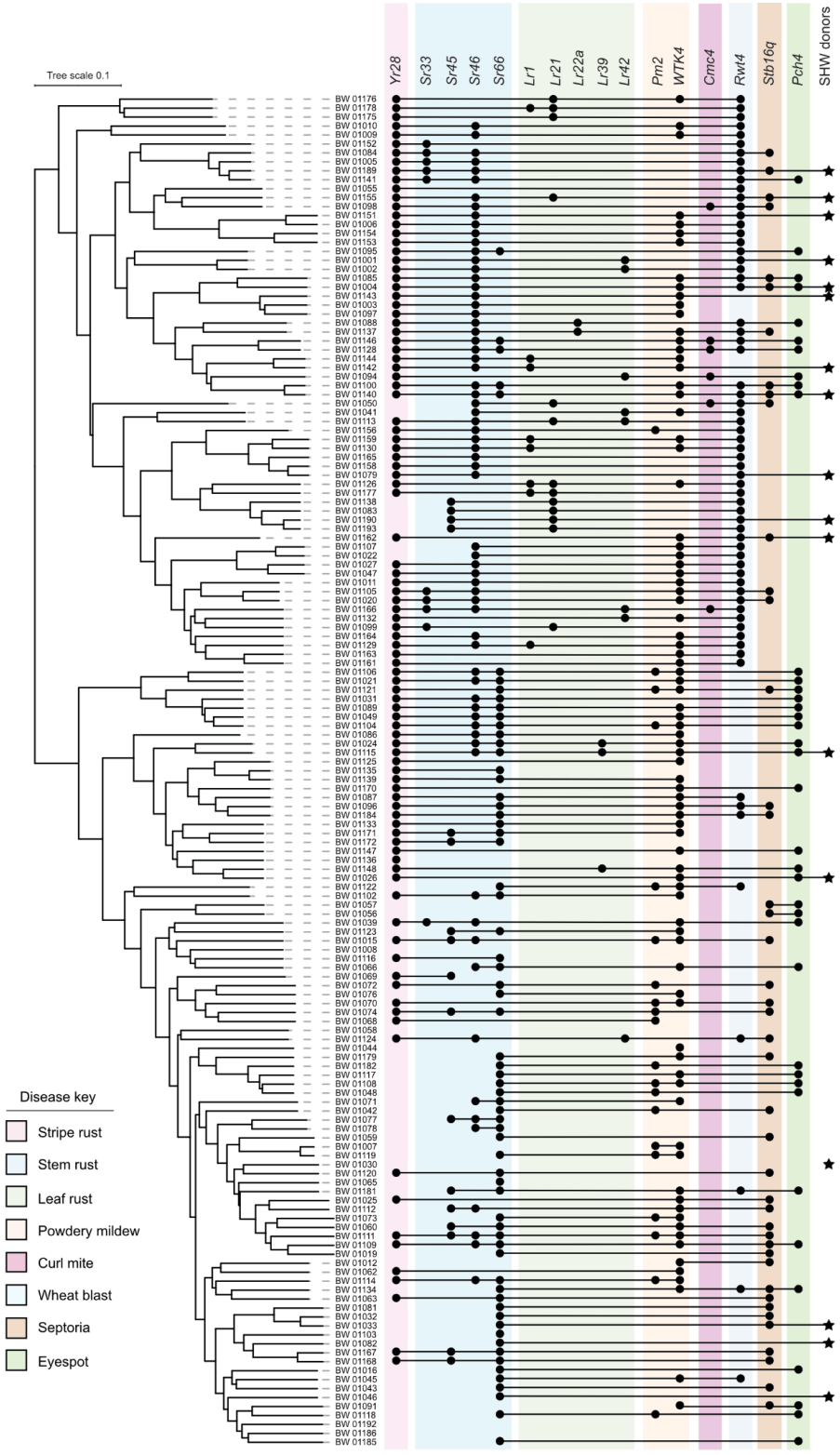

Figure 5

Genomics-assisted pyramiding of cloned *Ae. tauschii R* genes. Phylogenetic tree of the *Ae. tauschii* L2 diversity panel with black dots representing the predicted presence of a cloned *R* gene within an accession and stars indicating D subgenome donors used to create the NIAB synthetic hexaploids.

Supplementary Files

This is a list of supplementary files associated with this preprint. Click to download.

- supplementarytables.xlsx
- supplementaryfigures.pptx